Vol. 31 (2000) *ACTA PHYSICA POLONICA B* No 10–11

THE VECTOR MESON PRODUCTION IN PHOTOPRODUCTION ON HERA*

DUŠAN BRUNCKO

for H1 and ZEUS Collaboration

Institute of Experimental Physics SAS
Watsonova 47, Sk-043 53 Košice, Slovakia

(Received August 31, 2000)

A compilation of the last H1 and ZEUS results for vector meson production in photoproduction on HERA is presented.

PACS numbers: 13.60.Le, 25.20.Lj

1. Introduction

Production of Vector Mesons (VM) at HERA become a rich field of experimental and theoretical research. In this paper only fairly new results will be presented concentrating on the several properties of light and heavy mesons production. The appropriate overview of data on ρ, ω, $\psi(2S)$, J/Ψ, and Υ can be found in [1, 2, 4–6] and [3]. Vector meson can be produced elastically ($ep \to eVp$, where V denotes the vector meson) or in the proton dissociative channels $ep \to eVN$, where N denotes dissociative channels, which are born after proton breaks up into a low mass system.

2. Current picture of VM production at HERA

In Fig. 1 our present understanding of VM production is shown. The theoretical background for the selection of γp interactions ($Q \sim 0$ GeV^2) from ep one is based on WWA approximation [14]. From Fig. 1 follows two different scenarios — the light VM production, which can be described using VDM-like models based on the Regge phenomenology, see Fig. 2(a), and the heavy VM production, which today is better understood using models based on pQCD, see Fig. 2(b).

---

* Presented at the Meson 2000, Sixth International Workshop on Production, Properties and Interaction of Mesons, Cracow, Poland, May 19–23, 2000.

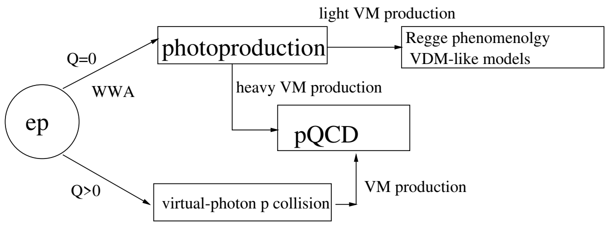

Fig. 1. The current picture of VM production in *ep* collisions at HERA.

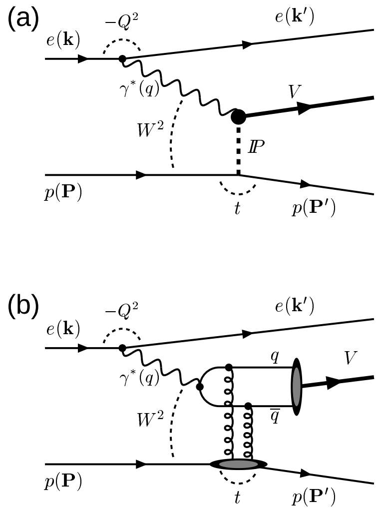

Fig. 2. (a) Non-perturbative models; (b) pQCD models.

2.1. Non-perturbative models

VDM-like models assume a simple linear form $\alpha(t) = \alpha_0 + \alpha' t$, where $\alpha(t)$ determines the dependence of the cross sections on the energy $W_{\gamma p}$ as $W_{\gamma p}^{4(\alpha(t)-1)}$. The values for the α_0 and α' are 1.02 and ~ 0.25 GeV^{-2}, respectively (soft Pomeron). The differential cross section $d\sigma/dt$ can be described using following formula

$$\frac{d\sigma}{dt} \sim \exp\left(-b|t|\right) \left(\frac{W}{W_0}\right)^{4(\alpha(t)-1)}, \tag{1}$$

where the slope b rises with W (*shrinkage*) as a

$$b = b(W) = b_0 + 4\alpha' \ln\left(\frac{W}{W_0}\right). \tag{2}$$

VDM-like models predict slow rise of cross section with W — $\sigma \sim W^{0.22\ldots0.32}$.

2.2. pQCD based models

Basic concept for models following from pQCD is factorization which has three stadia. At first one, before interaction with the proton, photon fluctuates into VM: $\gamma \to$ VM, at second one VM interacts with the proton and at last one we assume the formation of VM on the scale $\bar{Q}^2 = \frac{Q^2+M_V^2}{4}$. Cross section of VM production depends on energy W as a

$$\sigma(W) \propto |\bar{x}G(\bar{x},\bar{Q}^2)|^2\,, \quad \sigma(W) \propto W^{\delta}\,,$$

with $\bar{x} \propto \frac{\bar{Q}^2+M_V^2}{W_{\gamma p}^2}$ and $\delta \sim (0.80$–$1.00)$, where $xG(\bar{x},\bar{Q}^2)$ is gluon density in the proton. Therefore steeper rise with W reflects abundance of gluons at low x. For pQCD models *no shrinkage* is expected and because the transverse size of the $q\bar{q}$ is small, the typical value of b is near to 5 GeV^{-2} and we expect universal t-dependence with b.

2.3. Kinematics and observed channels

We measure (see Fig. 2a for the denotation of variables) $Q^2 = -q^2 = -(k-k')^2$, $t = (P-P')^2$, $W^2 = (q+P)^2$ and decay angles. The selection of γp events (in general: $Q^2 < 1$ GeV^2), *e.g.* for ZEUS is following: the Q^2 value ranges from the $Q^2_{\rm min} = M_e^2 y^2/(1-y) \approx 10^{-9}$ GeV^2, where M_e is the electron mass, to the value at which the scattered positron starts to be observed in the main detector $Q^2_{\rm max} \approx 1$ GeV^2, with $\langle Q^2\rangle \approx 5\times 10^{-5}$ GeV^2. The H1 typical values for J/ψ production are $\langle Q^2\rangle \approx 0.05$ GeV^2 and for $\varUpsilon$ production — $\langle Q^2\rangle \approx 0.11$ GeV^2. Common to all analyses are following observed (and used) decay modes: $\rho^0 \to \pi^+\pi^-$, $\omega \to \pi^+\pi^-\pi^0$, $\varPhi \to K^+K^-$, $J/\psi \to e^+e^-$, $J/\psi \to \mu^+\mu^-$, $\psi(2S) \to \mu^+\mu^-$ and $\psi(2S) \to J/\psi\pi^+\pi^-$, $\psi' \to e^+e^-$, $\psi' \to \mu^+\mu^-$ and $\varUpsilon \to \mu^+\mu^-$. For elastic selection we require no energy deposits in the main detector other than decay particles and the forward detectors were used to tag proton dissociative events.

3. Light VM production

In Fig. 3 $d\sigma/dM_{\pi\pi}$ for the elastic reaction $\gamma p \to \pi^+\pi^- p$ in the kinematic region $50 < W < 100$ GeV and $|t| < 0.5$ GeV^2 is shown. The asymmetric $\pi^+\pi^-$ spectrum can be properly described using the resonant contribution (dashed curve), the non-resonance $\pi^+\pi^-$ contribution (the dot-dashed curve) and with the contribution of the interference term (the dotted curve).

In Fig. 4 the t-dependence for ρ^0 and $\varPhi$ for the $\gamma p \to \rho^0(\varPhi)+Y$, $Y \sim$ dissociative system from p in the range $80 < W < 120$ GeV and $Q^2 < 0.01$ GeV^2 is shown. The t is measured by $t \simeq -p^2_{t,{\rm VM}}$, where $p^2_{t,{\rm VM}}$ is transverse momentum of VM. Looking on Fig. 4 we see that for ρ^0 non-perturbative contribution dominates, but for $\varPhi$ the situation is more complicated — pQCD models [7] can properly describe the shape only (for pQCD models the norm is not given).

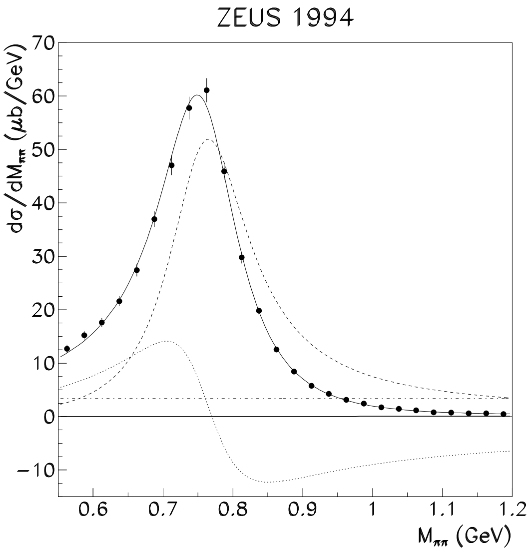

Fig. 3. ZEUS: $d\sigma/dM_{\pi\pi}$ for the elastic reaction $\gamma p \to \pi^+\pi^- p$ in the kinematic region 50 GeV $< W <$ 100 GeV and $|t| < 0.5$ GeV^2.

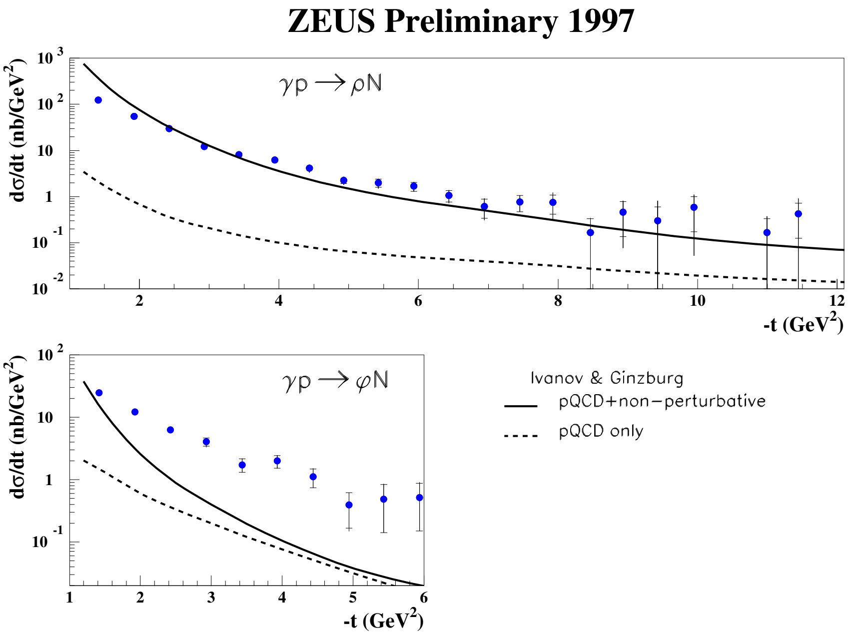

Fig. 4. The dissociative ρ^0 and Φ production.

The interesting picture rises for b value, which decreases with the increasing of the Q^2 value: $b_{\gamma p \to \rho^0 p} \sim 10$ GeV^{-2} for $|t| < 0.40$ GeV^2, $b_{\gamma p \to \rho^0 pY} \sim 6$ GeV^{-2} for $|t| < 0.50$ GeV^2, and $b_{\gamma^* p \to \rho^0 p} \sim 4.7$ GeV^{-2} for $Q^2 \sim 20$ GeV^2 — it means, for ρ^0 production the increasing Q^2 we go close to pQCD scenario. In Fig. 5 the elastic Φ meson production in γp dependence on $|t|$ and W is shown. From Fig. 5 we see that Φ production is connected with non-zero shrinkage and again, looking on $dN/dt \sim \exp(-b|t|)$, the b value decreases if Q^2 increases: $b = 7.3 \pm 1.0 \pm 0.8$ GeV^{-2} for $\langle Q^2 \rangle \sim 0$ GeV^2, $b = 5.8 \pm 0.5 \pm 0.6$ GeV^{-2} for $\langle Q^2 \rangle = 4.5$ GeV^2 and $b = 5.2 \pm 1.6 \pm 1.0$ GeV^{-2} for $\langle Q^2 \rangle = 10$ GeV^2.

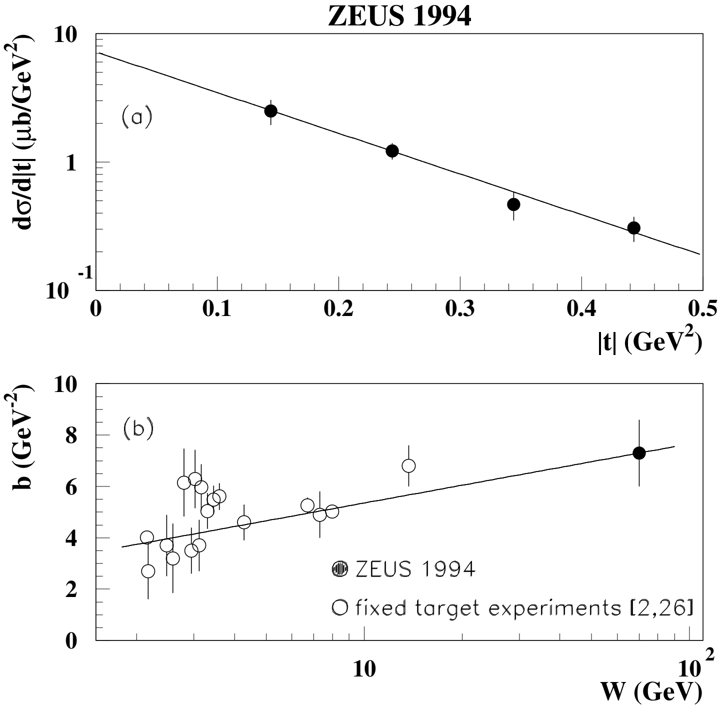

Fig. 5. The elastic cross section of Φ meson production in γp $d\sigma/d|t|$ on $|t|$ and W.

From Fig. 6 we see, that light VM production (ρ^0, ω, Φ) can be properly describe by VDM-like models. In Fig. 7 the shrinkage and $|t|$ study of ω production is presented. The value of b, $b = 10.0 \pm 1.2 \pm 1.3$ GeV^{-2}, indicates on the soft regime, but due to too large errors we cannot take conclusion about shrinkage presentation. Finally in Fig. 8 the exponential slopes b for VM in the photoproduction are shown. We clearly see decreasing of b with the mass of VM.

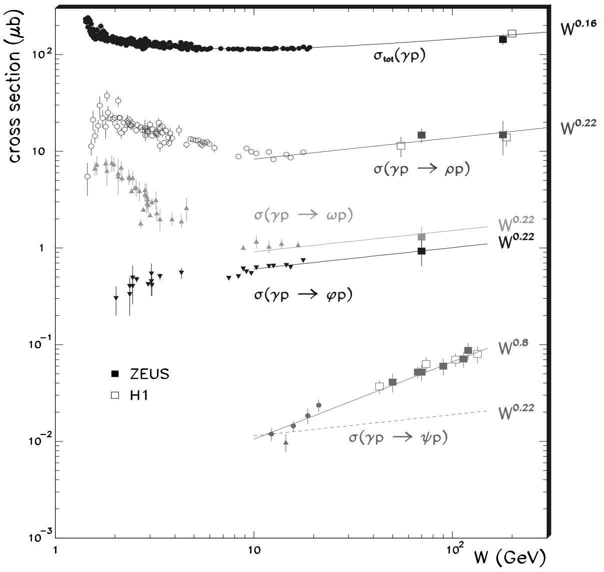

Fig. 6. The cross section dependence of VM production on W.

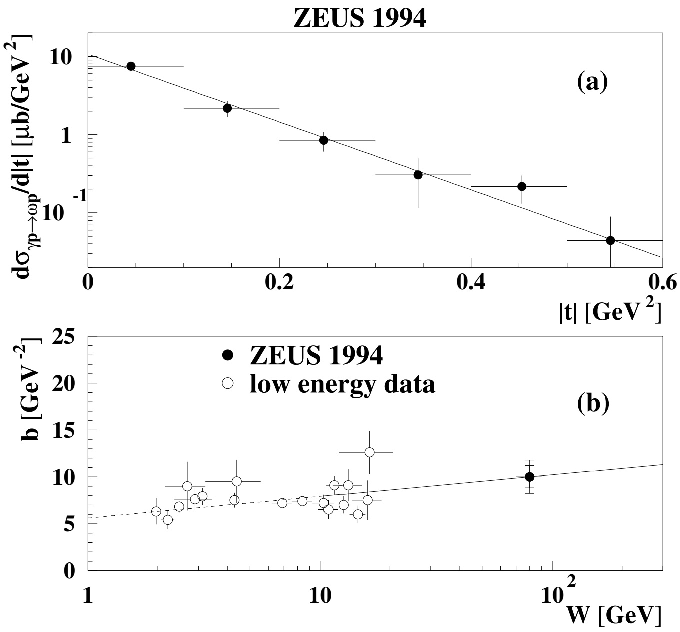

Fig. 7. The shrinkage and $|t|$ study of ω production.

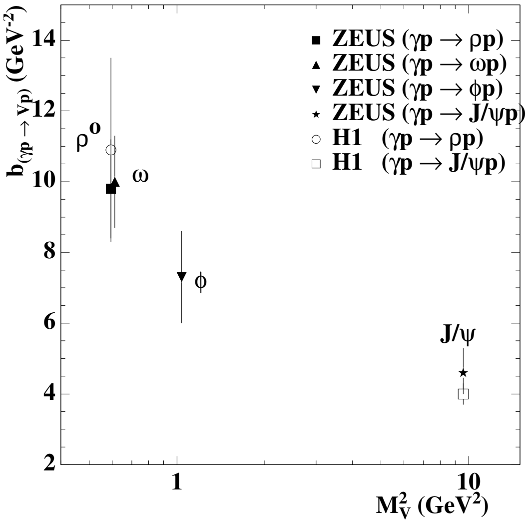

Fig. 8. The b value for VM in photoproduction.

4. Heavy VM production

4.1. J/Ψ photoproduction

It is interesting to compare prediction for J/Ψ in γp for VDM-like and pQCD models. In Fig. 9 the cross section of J/Ψ production in γp as a function of $W_{\gamma p}$ is shown. Curves represent pQCD model [8] with various gluon density distributions.

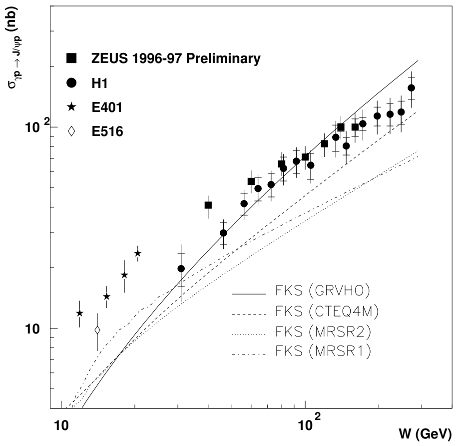

Fig. 9. The cross section of J/Ψ production in γp as a function of $W_{\gamma p}$.

The ZEUS collaboration measured the J/Ψ photoproduction cross section with proton dissociation at high $-t$. The measurement is shown in Fig. 10 together with a prediction within the BFKL framework by Bartels *et al.* [9]. A good description by the BFKL calculations is achieved. However, it has to be stressed that this is only a leading order calculation and that a large uncertainty is introduced due to the choice of α_s.

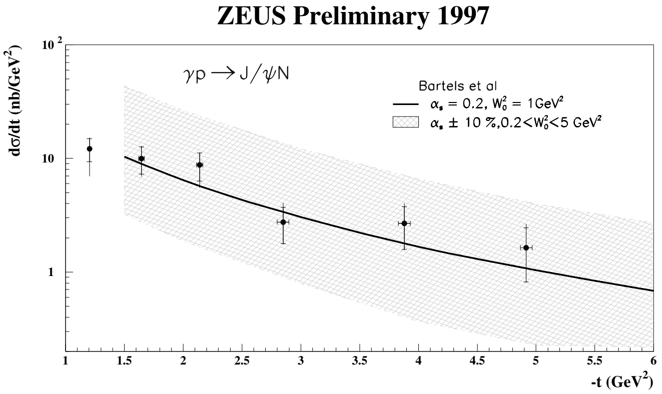

Fig. 10. J/Ψ photoproduction cross section with proton dissociation at high $-t$.

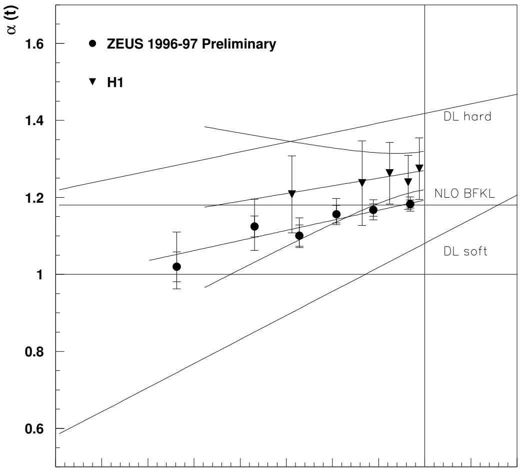

Fig. 11. The measured Regge trajectory $\alpha(t) = \alpha_o + \alpha' \cdot t$ for the process $\gamma p \to J/\Psi p$. The curves are explained in the text.

In Fig. 11 the measured Regge trajectory $\alpha(t) = \alpha_o + \alpha' \cdot t$ for the process $\gamma p \to J/\Psi p$ is shown. The highest curve corresponds to Donnachie–

Landshoff "hard" pomeron [11], the lowest one corresponds to Donnachie–Landshoff "soft" pomeron (usual soft pomeron), horizontal curve corresponds to NLO BFKL [10] prediction and lines around data shows the result of the fit. The fitted values are $\alpha(0) = 1.27 \pm 0.05$, $\alpha' = 0.08 \pm 0.17$ GeV^{-2} for H1 and $\alpha(0) = 1.193 \pm 0.011^{+0.015}_{-0.010}$, $\alpha' = 0.105 \pm 0.024^{+0.022}_{-0.020}$ GeV^{-2} for ZEUS, respectively. In next Fig. 12 the extraction of $\alpha'_{I\!P}$ (using formula $b(W) = b_0 + 4\alpha'_{I\!P} \ln(\frac{W}{W_0})$) from ZEUS data is shown. The result $\alpha'_{I\!P} = 0.098 \pm 0.035(\mathrm{stat}) \pm 0.050(\mathrm{syst})$ GeV^{-2} is too far from soft pomeron value.

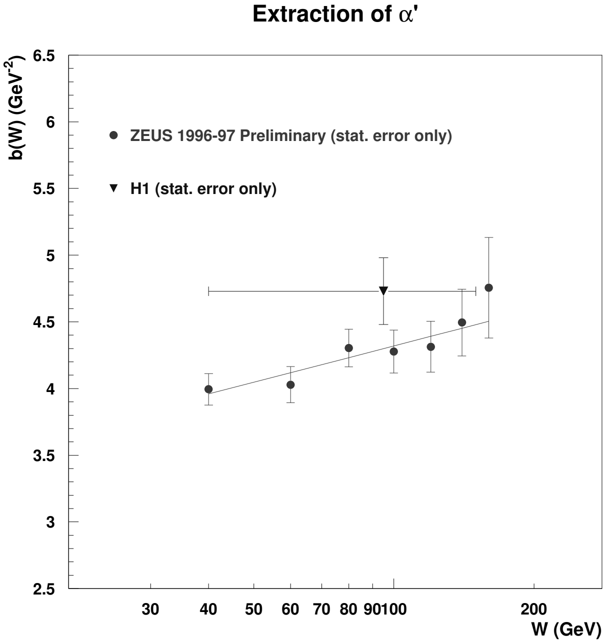

Fig. 12. The $b(W)$ dependence on W.

4.2. ψ' production in γp

In Fig. 13 the dependence of the ratio $\frac{\sigma_{\psi'}}{\sigma_{J/\psi}}$ on the energy W is shown. From Color Singlet Model (CSM) follows the independence of $\frac{\sigma_{\psi'}}{\sigma_{J/\psi}}(W)$ on W and this is confirmed by data. The calculation using CSM are at LO level only and the error due to the uncertainty of $\Gamma_{\psi' \to l^+l^-}$ is not included. Now we can conclude that within the present statistics the inelastic ratios are consistent with the elastic ones and the ratio of inelastic ψ' to J/ψ in γp is in agreement with expectation in the CSM.

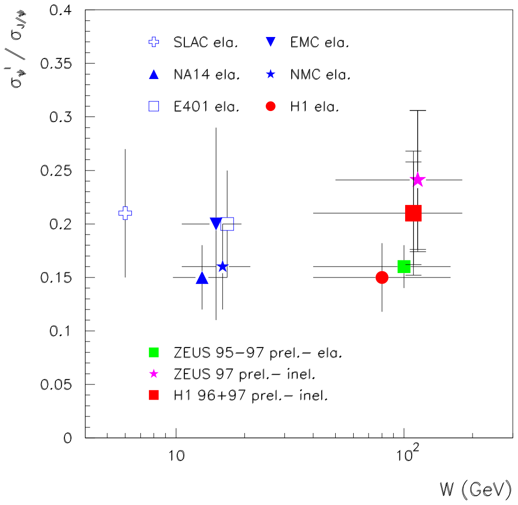

Fig. 13. The dependence of $\frac{\sigma_{\psi'}}{\sigma_{J/\psi}}$ on the energy W.

4.3. Elastic Υ photoproduction

In Fig. 14 the $\mu^+\mu^-$ spectrum together with the region where we expect of Υ production is shown. Full line represents dominated Bethe–Heitler background. We see indication on Υ production, but we do not distinguished among $\Upsilon(1S)$, $\Upsilon(2S)$ and $\Upsilon(3S)$ resonances. In Fig. 15 the dependence of cross section of Υ photoproduction on the energy $W_{\gamma p}$ is shown, where only the results from pQCD calculations are presented [12,13]. We conclude that the recent measurements of elastic Υ photoproduction are in good agreement with theoretical expectations of pQCD.

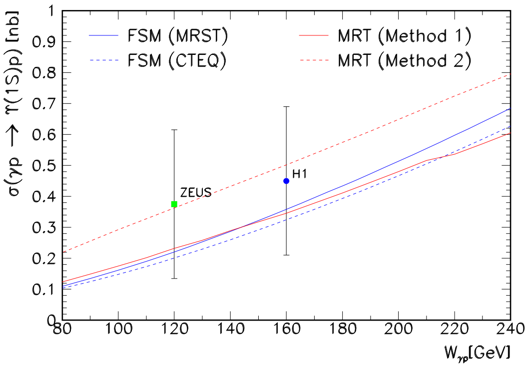

Fig. 14. The dependence of Υ photoproduction on $W_{\gamma p}$.

5. Some general characteristics of VM photoproduction

When Q^2 increase the exchanged photon acquires a longitudinal component. The ratio $R = \sigma_{\rm L}/\sigma_{\rm T}$ has been measured for various VM — see *e.g.* Fig. 15(a), where the ratio R is shown for the elastic $\varPhi$ meson as a function of Q^2 and is seen to increase (the R rises steeply at small Q^2 and a weaker at large Q^2). In Fig. 15(b) the dependence of ratio R for the elastic ρ, $\varPhi$ and $J/\varPsi$ on Q^2/M_V^2 is shown. The increase of R can be seen with Q^2/M_V^2.

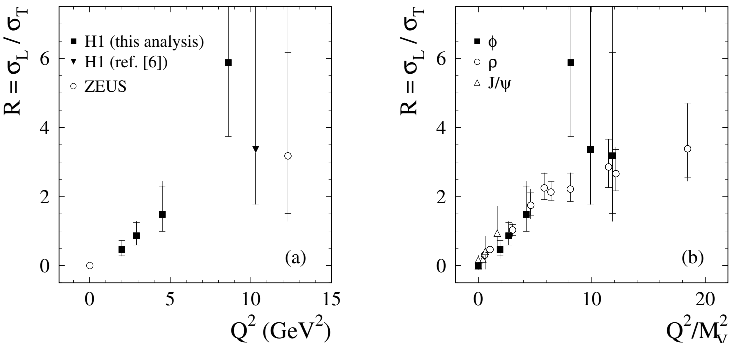

(a) (b)

Fig. 15. (a) The dependence of ratio R for the elastic $\varPhi$ meson on Q^2; (b) The dependence of ratio R for the elastic VM on Q^2/M_V^2.

Due to quarks charges counting and the quark composition of the wave function (SU(5) group) for VM production we expect following ratio: $\rho^0 : \omega : \varPhi : J/\psi : \varUpsilon = 9 : 1 : 2 : 8 : 2$. It is interesting to look on data for such behavior. In Fig. 16 the dependence of the ratio of cross sections for $\varPhi/J/\varPsi$ and ρ photoproduction in the dissociative channels on $-t$ is shown. SU(5) symmetry for $J/\varPsi$ photoproduction is restored at large Q^2. Analogical behavior for the dependence of the elastic VM photoproduction on Q^2 in Fig. 17 is shown. From Fig. 17 could be observed that the ratio $\varPhi/\rho$ is badly broken for $Q^2 \sim 0$ GeV^2 and for ω the flat is seen which perhaps can be interpreted as a mass effect.

Finally, in Fig. 18 the integrated cross sections for VM scaled by the SU(5) ratios as a function of $Q^2 + M_V^2$ is shown. The data are scaled to $W_{\gamma p} = 75$ GeV and are seen to agree well with each other and can be fitted to the ρ data. We can conclude that within present errors $Q^2 + M_V^2$ is a good scale for photoproduction of VM at low values of t.

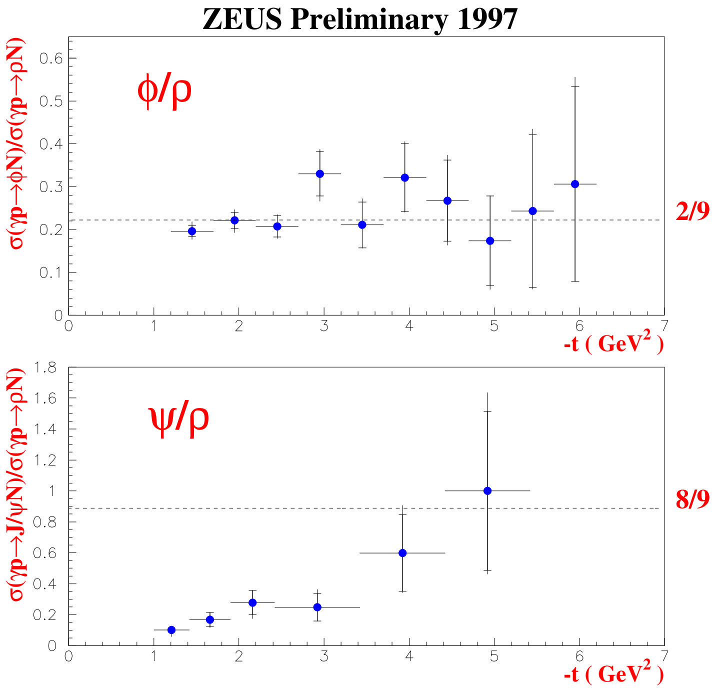

Fig. 16. The ratio of cross sections for Φ and ρ (up picture) and the ratio of cross sections for J/Ψ and ρ photoproduction (down picture) in the dissociative channels on $-t$.

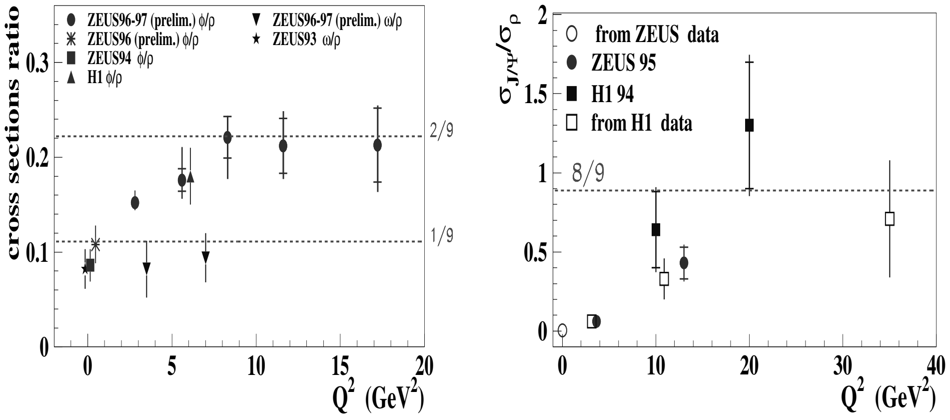

Fig. 17. The dependence of the ratio of elastic cross sections for VM and ρ in photoproduction on Q^2.

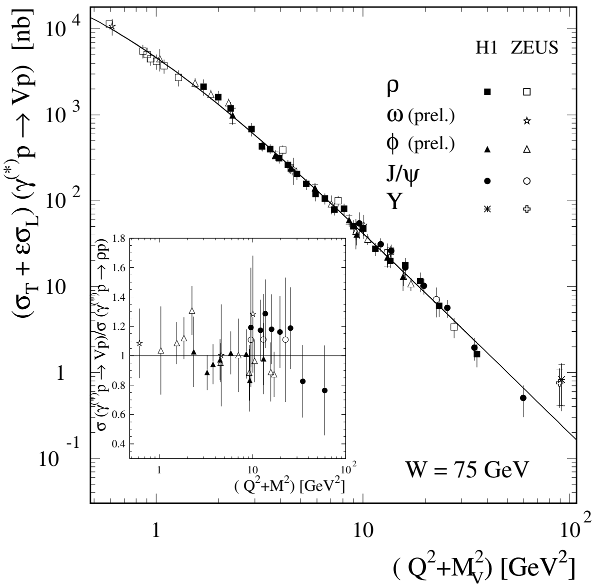

Fig. 18. The integrated cross sections for VM scaled by the SU(5) ratios as a function of $Q^2 + M_V^2$ is shown.

I thank the organizers for the possibility to present H1 and ZUES results and for the invariable forbearance for my contribution.

REFERENCES

[1] ZEUS Collaboration, J. Breitweg *et al.*, DESY 00-084 (June 2000), accepted by *Phys. Lett.* **B**; ZEUS Collaboration, M. Derrick *et al.*, *Z. Phys.* **C73**, 73 (1996).

[2] ZEUS Collaboration, J. Breitweg *et al.*, DESY 99-102 (July 1999); ZEUS Collaboration, J. Breitweg *et al.*, *Eur. Phys. J.* **C2**, 247 (1998); ZEUS Collaboration, M. Derrick *et al.*, *Z. Phys.* **C69**, 39 (1995); ZEUS Collaboration, M. Derrick *et al.*, *Phys. Lett.* **B356**, 601 (1995); H1 Collaboration, C. Adloff *et al.*, *Eur. Phys. J.* **C13**, 371 (2000); H1 Collaboration, S. Aid *et al.*, *Nucl. Phys.* **B463**, 3 (1996).

[3] ZEUS Collaboration, J. Breitweg *et al.*, DESY 98-089 (July 1998).

[4] ZEUS Collaboration, J. Breitweg *et al.*, *Z. Phys.* **C76**, 599 (1997); ZEUS Collaboration, J. Breitweg *et al.*, *Z. Phys.* **C75**, 215 (1997); H1 Collaboration, C. Adloff *et al.*, *Phys. Lett.* **B483**, 23 (2000); H1 Collaboration, S. Aid *et al.*, *Nucl. Phys.* **B472**, 3 (1996).

[5] ZEUS Collaboration, M. Derrick *et al.*, *Phys. Lett.* **B380**, 220 (1996); ZEUS Collaboration, M. Derrick *et al.*, *Phys. Lett.* **B377**, 259 (1996); H1 Collaboration, C. Adloff *et al.*, *Phys. Lett.* **B483**, 360 (2000).

[6] H1 Collaboration, C. Adloff *et al.*, *Phys. Lett.* **B421**, 385 (1998).

[7] I.F. Ginzburg, D.Yu. Ivanov, *Phys. Rev.* **D54**, 5523 (1996).

[8] L.L. Frankfurt, W. Koepf, M. Strikman, *Phys. Rev.* **D57**, 512 (1998).

[9] J. Bartels *et al.*, *Phys. Lett.* **B375**, 301 (1996).

[10] S.J. Brodsky *et al.*, *JETP Lett.* **70**, 155 (1999).

[11] A. Donnachie, P.V. Landshoff, *Phys. Lett.* **B348**, 213 (1995); *Phys. Lett.* **B347**, 408 (1998).

[12] L.L. Frankfurt, M.F. Dermott, M. Strikman, *JHEP* **002**, 9902 (1999).

[13] A.D. Martin, M.G. Ryskin, T. Teubner, *Phys. Lett.* **B454**, 339 (1999).

[14] C.F. Weizsäcker, *Z. Phys.* **88**, 612 (1934).